

3aBB7. Aberration-corrected time-domain ultrasound diffraction tomography. T. Douglas Mast (Appl. Res. Lab., Penn State Univ., University Park, PA 16802)

The inverse scattering problem of reconstructing a spatially dependent sound speed variation from far-field time-domain acoustic scattering measurements is considered. Such reconstructions are quantitative images with applications including ultrasonic mammography. Although the linearized time-domain inverse scattering problem is shown to have no general solution for finite signal bandwidth, an approximate solution to the linearized problem is constructed using a simple delay-and-sum method analogous to "gold standard" ultrasonic beamforming. The form of this solution suggests that the full nonlinear inverse scattering problem can be approximated by applying appropriate angle- and space-dependent time shifts to the time-domain scattering data; this analogy leads to a general approach to aberration correction. Two related methods for aberration correction are presented: one in which delays are computed from estimates of the medium using an efficient straight-ray approximation, and one in which delays are applied directly to a time-dependent linearized reconstruction. Numerical results indicate that these correction methods achieve substantial quality improvements for imaging of large scatterers. [Work supported by the Breast Cancer Research Program of the U.S. Army Medical Research and Materiel Command.]

10:45

3aBB8. Theoretical considerations for the use of microbubbles as point targets for phase aberration correction. Dimitris Psychoudakis (Elec. Eng. and Computer Sci., Univ. of Michigan, Ann Arbor, MI 48109-2122), J. Brian Fowlkes, John L. Volakis, Oliver D. Kripfgans, and Paul L. Carson (Univ. of Michigan, Ann Arbor, MI 48109-0553)

Bubbles can be produced by vaporization of perfluorocarbon droplets of a few μm diameter. These bubbles can reach up to 100 μm in diameter and their backscatter is calculated to be more than 10 dB above that of several organ tissues. At these sizes and for diagnostic frequencies (2–8 MHz), bubbles can be approximated by the nonrigid sphere scattering solution employed here. This presentation concerns the bubble size and its implications on the backscatter amplitude and the phase error introduced in diagnostic ultrasound when assuming that the bubble acts as a point target for phase aberration correction. The phase error is the difference between the phase at each location along the receiving aperture relative to that at the aperture center, compared with the same relative phase for a perfect point target. Evaluations were made of the phase error with respect to a range of transducer f -numbers (0.5–2.0) for a specific bubble size (30 μm radius) and at certain frequencies (2–8 MHz). For example, at 5 MHz the phase error introduced by the point target assumption is maximally 5 deg, while the phase error of breast tissue scattering is around 160 deg. [Work supported by PHS Grant No. R01HL54201 from the National Heart, Lung, and Blood Institute.]

11:00

3aBB9. Comparison between time reversal and spatio-temporal inverse filter application to focusing through a human skull. Mickael Tanter, Jean-Francois Aubry, Jean-Louis Thomas, and Mathias Fink (Laboratoire Ondes et Acoustique, ESPCI, Paris VII Univ., Paris, France)

Ultrasonic imaging systems capabilities are strongly dependent on the focusing quality of the ultrasonic beam. In the case of brain imaging, the skull strongly degrades the ultrasonic focusing pattern by introducing strong phase and amplitude aberrations of the wave-front. In previous work, this degradation of the beam focus had been partially corrected by coupling the time reversal focusing process to an amplitude compensation of the emission signals. In that case, the optimal focus was reproduced down to –20 dB, but the sidelobe level remained at about –25 dB. This elegant technique will be compared to another focusing technique recently developed in our laboratory, called spatio-temporal inverse filtering. Thanks to this method, based on the inversion of the propagation operator at each frequency within the bandwidth of our transducers, experimental focusing through the skull is now comparable to optimal focusing in a

homogeneous medium. Those two methods not only differ theoretically, but also suffer differently from all the experimental defects, such as the limited bandwidth of the transducers or the limited aperture of the arrays. A comparison of the results obtained with both techniques in water and through a human skull clearly highlights the advantages and the drawbacks of each method.

11:15

3aBB10. Integrated matrix arrays. Ken Erikson, Jason Stockwell, and Robert McPhie (BAE Systems, P.O. Box 868, Nashua, NH 03061-0868)

Improved image quality requires the use of matrix ($n \times m$) arrays with a thousand or more elements. As element numbers increase and their dimensions grow smaller, limitations to present fabrication technologies arise. Cost, ergonomics, produceability, and reliability are important issues. Signal loss due to the capacitance of interconnecting coax cables becomes a fundamental problem. Connecting an integrated circuit directly to the array elements alleviates all these problems. Each unit cell of such a custom transmitter/receiver integrated circuit (TRIC) may have high voltage switches for transmitting; a preamplifier which minimizes signal loss due to capacitance in coax cables and a multiplexer to send the array signals over fewer wires. Additional signal processing and beam forming may also be included. Issues with currently available arrays are reviewed. The new technology for direct connection of arrays to IC's is described. The paper concludes with speculation about future possibilities of this approach.

11:30

3aBB11. Measurements of the spatial coherence of the fundamental and second-harmonic beams for a clinical imaging system. Russell J. Fedewa, Kirk D. Wallace, Mark R. Holland (Lab. for Ultrason., Dept. of Phys., Washington Univ. of St. Louis, One Brookings Dr., St. Louis, MO 63130), James R. Jago, Gary C. Ng, Matthew R. Rielly, Brent S. Robinson (ATL Ultrasound, Bothell, WA 98041-3003), and James G. Miller (Lab. for Ultrason., Washington Univ. of St. Louis, St. Louis, MO 63130)

Spatial coherence of backscattered signals underlies correlation-based phase aberration corrections. The van Cittert–Zernike theorem relates frequency-independent spatial coherence to the autocorrelation of the transmit apodization. Previous studies suggest that the mainlobe of the nonlinearly generated harmonic beam is wider and exhibits lower sidelobes than a beam linearly generated at the harmonic frequency. The objective of this study was to measure the spatial coherence associated with fundamental and nonlinearly generated harmonic beams. Using data experimentally acquired from a clinical scanner (ATL HDI5000), two independent methods were employed to measure the spatial coherence. One approach measured the spatial coherence of backscatter from a tissue-mimicking phantom using rf signals from individual elements of a linear array. In the second approach, the effective apodization was determined by a linear angular spectrum backpropagation of hydrophone-sampled data from a transverse plane in the focal zone. The results show that the effective apodization of the nonlinearly generated harmonic beam is more aggressive than the actual transmit apodization. The spatial coherence associated with the second-harmonic beam differs from the spatial coherence of the fundamental beam, but is predicted by the effective apodization. [Supported in part by NIHHL40302 & ATL.]

11:45

3aBB12. Efficient computation of field of 2-D array with limited diffraction array beams. Jian-yu Lu and Jiqi Cheng (Ultrasound Lab, Dept. of Bioengineering, The Univ. of Toledo, Toledo, OH 43606, jilu@eng.utoledo.edu)

Two-dimensional (2-D) arrays are useful for improving quality of three-dimensional (3-D) medical imaging in ultrasound. Beams produced with a 2-D array are usually simulated with the Rayleigh–Sommerfeld diffraction formula (RSDF). In general, the RSDF requires a 2-D integra-

tion for each field point in space and thus is very time consuming. Fresnel approximation may reduce the 2-D integration to 1-D but will not yield satisfactory results near the transducer surface or for field at a large angle from the beam axis. In this work, limited diffraction array beams are used to synthesize beams produced with a 2-D array [J.-Y. Lu, *Int. J. Imaging Syst. Technol.* **8**, 126–136 (1997)]. In this method, the 2-D integration is

replaced with a 2-D summation leading to a much faster computation. The method is accurate even if the field to be evaluated is very close to the surface of a transducer. Results of Bessel beams, X waves, and focused Gaussian beams will be shown and compared with those obtained with the RSDF and the experiments. [This work was supported in part by Grant No. HL60301 from the National Institutes of Health of the U.S.A.]

WEDNESDAY MORNING, 6 JUNE 2001

PARLOR B, 8:00 TO 10:05 A.M.

Session 3aEA

Engineering Acoustics: Acoustic Devices and Systems

Elizabeth A. McLaughlin, Chair

Naval Undersea Warfare Center, Code 2132, 1176 Howell Street, Newport, Rhode Island 02841-1708

Chair's Introduction—8:00

Contributed Papers

8:05

3aEA1. A PVDF long time-constant force sensor. Aaron M. Foulk and W. Jack Hughes (Appl. Res. Lab., Penn State Univ., P.O. Box 30, State College, PA 16804, wjh2@psu.edu)

A low-profile large-area underwater force sensor was desired to measure quasistatic forces on a rigid structure. The design for a PVDF sensor (a low-profile piezoelectric) intended for use in measuring sustained (10-s) impact forces with minimal error is presented. The final sensor design integrates a PVDF bimorph piezoelectric element and long time constant charge amplifier electronics into a 1-in. diam by 3/8-in. waterproof package. This work addresses design issues including electronics design to maximize the useful time constant, piezoelectric material selection, thermal design and simulation to minimize pyroelectric effects and noise minimization efforts. [This work was supported by NSWC-CD and ONR.]

8:20

3aEA2. Modulated piezoresistive sensor for airborne infrasound. Thomas B. Gabrielson (Appl. Res. Lab., The Penn State Univ., P.O. Box 30, State College, PA 16804)

This paper will describe the design, construction, and testing of a piezoresistive sensor for airborne acoustics in the frequency range 0.005–100 Hz. Intended as a candidate for many-element infrasound arrays where element cost is critical, the sensor was designed around an inexpensive silicon-membrane chip with an implanted piezoresistive bridge. The prototype has a measured self-noise below one millipascal per root hertz at 1 Hz with a $1/f$ power spectrum to 0.005 Hz, the designed low-frequency rolloff. The responsivity is nominally 20 mV/Pa with a linear signal range to 150 Pa. When the bridge is operated with high-frequency drive and synchronous detection, the self-noise is within a factor of 2 of the intrinsic Johnson noise of the resistive bridge. This self-noise level is well below ambient levels in the microbarometric region from 0.2 to 0.7 Hz. Basic sensor-element limitations will be discussed along with the electronics and package design. In addition, the techniques for calibration and self-noise evaluation will be presented. [Work sponsored by the U.S. Army Space and Missile Defense Command.]

8:35

3aEA3. The determination of the depth to the liquid-gas interface in a producing well. Elmer L. Hixson, Augusto L. Podio, and Fernando Garcia-Osuno (Univ. of Texas, Austin, TX 78712)

Many oil wells use electrically driven pumps at the bottom of the well to pump oil to the surface. If the oil-gas interface falls below the pump, gas is pumped, the pump overheats and usually fails. A passive acoustic system is described here that uses the annulus between the production tubing and the cemented steel casing as a closed end gas filled tube. Pump noise excites many longitudinal resonant modes. These modes occur at n -half wavelengths of the tube length. The depth is then related to the sound speed in the gas and the difference frequency between modes as measured by a microphone at the top of the well and a spectrum analyzer. When the depth falls below a critical value as indicated by a minimum frequency, the pump is turned off.

8:50

3aEA4. A new hand-held meter for measuring the occlusion effect produced by, and leakage around, earmolds. Mead C. Killion and Jack Goldberg (Etymotic Research, 61 Martin Ln., Elk Grove Village, IL 60007, abonso@aol.com)

Three of the most common complaints by hearing aid wearers are (a) difficulty hearing in noise, (b) the occlusion effect (hollow voice sound), and (c) feedback. The latter two can be largely controlled by earmold construction. What has been lacking is a simple way to measure earmold performance with regard to those two properties. A new hand-held occlusion effect meter using a 0.4-mm-thick crescent-shaped probe tube will be described.

9:05–9:20 Break

9:20

3aEA5. Research into the comfortable volume control curve of TV in Korean style apartments. Ki Duk Kim (Quality and Reliability Lab., Daewoo Electron. Co., Ltd., 412-2, Chongchun2-Dong, Pupyung-Ku, Incheon, Korea, soundexpert@korea.com), Chul Whan Kim, Hoon Ki Choi, and Dong Su Ryu (Daewoo Electron. Co., Ltd., Pupyung-Ku, Incheon, Korea)

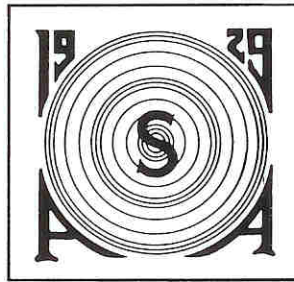
We occasionally experience anger because of unsuitable TV volume for comfortable and clear listening. We do not concentrate on TV while annoyed that we are not tuned in at the desired sound volume. Therefore, we made the preference volume width in watching TV with consideration

The Journal of the Acoustical Society of America

6/5/01
Jian-yu Lo

Vol. 109, No. 5, Pt. 2 of 2, May 2001

<http://asa.aip.org>



**141st Meeting
Acoustical Society of America**

**Palmer House Hilton Hotel
Chicago, Illinois
4-8 June 2001**

Table of Contents on p. A5